BORON-OXYGEN DEFECTS IN COMPENSATED P-TYPE CZOCHRALSKI SILICON

D. Macdonald[1], A. Liu[1], F. Rougieux[1], A. Cuevas[1], B. Lim[2], J. Schmidt[2], M. Di Sabatino[3] and L. J. Geerligs[4]
[1]School of Engineering, The Australian National University, Canberra ACT 0200, Australia.
[2]ISFH, Am Ohrberg 1, D-31860 Emmerthal, Germany.
[3]SINTEF Materials and Chemistry, A. Getz v. 2B, 7465 Trondheim, Norway.
[4]ECN Solar Energy, PO Box 1, NL-1755 ZG Petten, The Netherlands.
email: daniel.macdonald@anu.edu.au

ABSTRACT: The extent of formation of the well-known boron-oxygen defect has been measured in deliberately compensated p-type Czochralski silicon. Both the defect concentration and the defect formation rate confirm recent results showing that the amount of boron-oxygen defects formed is determined by the net doping $p_0=N_A-N_D$, rather than the total boron concentration N_A. The presence of boron-phosphorus pairs has been postulated previously as a possible explanation for this effect. However, we find that the existence of such pairs is not consistent with measurements of the majority carrier mobility, and the crossover point of interstitial iron/iron-boron pairs in compensated silicon. However, whatever the cause of the reduced impact of oxygen-boron defects in compensated silicon, the implications for solar cells made with compensated feedstock are positive.
Keywords: defects, recombination, Czochralski silicon.

1 INTRODUCTION

Significant levels of dopant compensation are likely to occur in new forms of solar-grade silicon feedstocks. The existence of additional boron in compensated *p*-type silicon raises the prospect of increased recombination due to the presence of the well-known boron-oxygen defect [1], which could make the use of such material for solar cells less attractive. However, a very recent study [2] has indicated that the extent of this defect is in fact not determined by the total concentration of boron acceptors N_A in a wafer, but by the net doping $p_0=N_A-N_D$, leading to the postulation of boron-phosphorus pairs (B-P) in compensated wafers. These previous studies were based on voltage measurements of cells made with feedstock containing a mixture of pure and upgraded silicon, which may also contain other impurities.

The aim of this work is to systematically study the generation of boron-oxygen defects in deliberately compensated Czochralski-grown silicon that is otherwise extremely pure. The concentration of boron-oxygen defects is measured directly via carrier lifetime measurements on compensated and non-compensated wafers of similar net doping, giving a direct comparison. The rate at which the defects are formed under illumination is also reported. Combining these measurements allows us to confirm that the defect concentration is indeed determined only by the net doping. However, we find that the proposed presence of B-P pairs is not consistent with our measurements of the majority carrier mobilities, or the position of the characteristic lifetime 'crossover point' caused by the dissociation of iron-boron pairs.

2 EXPERIMENTAL METHODS

The samples used were cleaved sections of 155×155 mm pseudo-square, *p*-type, <100>-oriented Czochralski-grown silicon (Cz-Si) wafers. There were wafers from three boron-doped control ingots (non-compensated), and two compensated ingots, doped with both boron and phosphorus. The amounts of dopant added to the melt are shown in Table I. High-purity feedstock and dopant sources were used, hence we do not expect significant quantities of unintended dopants.

The interstitial oxygen concentrations $[O_i]$ were measured by FTIR, and were between 9.4×10^{17} and 1.1×10^{18} cm^{-3}, and hence very similar from wafer to wafer. FZ controls with low oxygen content were also included in the experiment. Samples were initially subject to a phosphorus diffusion step to remove fast-diffusing metal impurities such as interstitial iron, which can otherwise make determination of the boron-oxygen defect concentration difficult. The high temperature associated with the phosphorus gettering also eliminates any unwanted thermal donors in the Cz-Si [3].

After etching the gettering layer, all samples were coated at 400°C with PECVD SiN for surface passivation. Effective carrier lifetimes were measured with the Quasi-Steady-State Photoconductance technique (QSSPC) [4]. Lifetime measurements were performed prior to any boron-oxygen defect activation, referred to as $\tau_{annealed}$. The lifetime was measured again after 5 days of illumination under a halogen lamp with an intensity equivalent to approximately one tenth of a sun, more than sufficient to fully activate the defect. This final lifetime is denoted as $\tau_{degraded}$. The relative defect concentration N_t^* can then be determined via $N_t^*=1/\tau_{degraded}-1/\tau_{annealed}$, where the carrier lifetimes are measured at an excess carrier density equal to 10% of the net doping p_0.

The resistivity of the gettered wafers is shown in Table I. Table I also shows independent measurements of the boron and phosphorus concentrations N_A and N_D at the wafer level by Glow-Discharge Mass Spectrometry (GDMS), performed at SINTEF [5]. N_A was also determined by the recently proposed technique based on measuring the iron-acceptor pair association time-constant τ_{assoc} [6].

3 RESULTS AND DISCUSSION

3.1 The net doping

A key parameter for the analysis below is the net doping p_0. It could, in principle, be estimated by

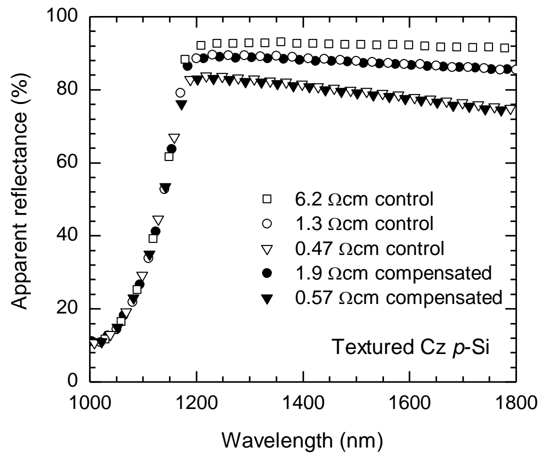

Figure 1. Reflectance as a function of wavelength measured on textured wafers.

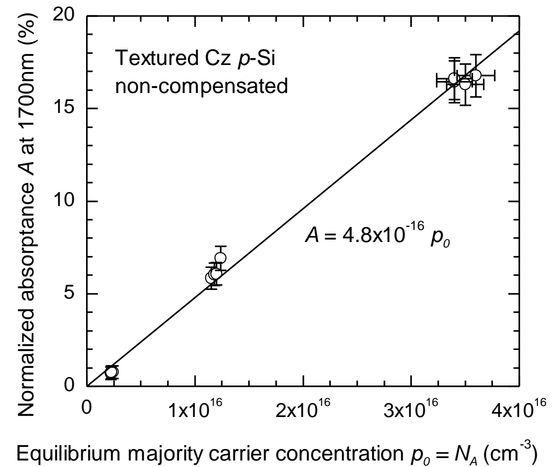

Figure 2. Normalized absorptance at 1700 nm as a function of p_0 for the control samples. The solid line is a linear fit to the data.

subtracting the boron and phosphorus concentrations determined by GDMS, but this may be rather inaccurate when the compensation is strong, as is the case here. Resistivity measurements alone are not sufficient, since the majority carrier mobility is affected by compensation to a degree that is not well known. In this work we have used Free-Carrier Absorption (FCA) to estimate p_0 in the compensated samples, by direct comparison to the FCA observed in the non-compensated controls. Capacitance – voltage measurements are an alternative approach.

Figure 1 plots the reflectance R measured with a spectrophotometer, as a function of wavelength, for textured samples from each ingot. Figure 2 shows the normalised absorptance at 1700 nm for the non-compensated samples only, as a function of p_0 (determined from the resistivities), as described in detail elsewhere [7]. The result is a linear relationship between p_0 and the normalized absorptance, as shown by the straight line in Figure 2. By measuring the absorptance in the compensated samples, we used this linear fit to estimate the p_0 for those samples also (shown in Table I).

We then determined the majority carrier (hole) mobility for the compensated samples, via the resistivity ρ and p_0 measurements, using $1/\rho = q\,\mu_h\,p_0$. The results were μ_h=319±40 and 303±30 cm^2/Vs for ingots 45 and 44 respectively. These may be compared with the predicted hole mobilities from Klaassen's model [8,9], using as input parameters the N_A values estimated from the iron-acceptor pair association time-constant τ_{assoc}, and N_D values determined via $N_D = N_A - p_0$. Note that Klaassen's model accounts for the different scattering cross sections of minority and majority dopant atoms, and so should in principle be applicable to compensated silicon. The model predicts mobilities of μ_h = 347 and 307 cm^2/Vs for ingots 45 and 44 respectively (assuming a temperature of 304K), in good agreement with our measured mobility values above. These results imply that Klaassen's model yields reasonable estimates of the majority carrier mobilities in the compensated samples. We therefore also used it to estimate the electron mobility, thus yielding the mobility sum $\mu_h+\mu_e$ required for QSSPC lifetime measurements on compensated samples.

3.2 The defect concentration

Armed with appropriate mobility sums, we are then able to measure the QSSPC carrier lifetimes for both the non-compensated and compensated samples. These are shown in Figure 3, with all lifetimes reported at an excess carrier density equal to 10% of the net doping p_0. After degradation, the lifetimes are reduced by approximately an order of magnitude in both the compensated and non-compensated Cz wafers. These lifetimes are subsequently used to determine the boron-oxygen defect concentration N_t*. The results are shown in Figure 4. For the non-compensated control samples, the defect concentration increases approximately linearly with the boron concentration N_A, as expected. The N_t^* values for the compensated samples are shown plotted as a function of

Table I. *Some parameters for the five ingots studied: boron and phosphorus concentrations added to the melt, measured resistivities, the boron and phosphorus concentrations N_A and N_D in the wafers determined by GDMS, N_A measured via the iron-acceptor re-pairing time constants τ_{assoc}, the net doping p_0 measured by FCA, and the donor concentration determined by $N_D = N_A - p_0$.*

Ingot	Boron added to melt (cm^{-3})	Phos. added to melt (cm^{-3})	Measured resistivity ρ (Ωcm)	N_A from GDMS (cm^{-3})	N_D from GDMS (cm^{-3})	N_A from τ_{assoc} (cm^{-3})	p_0 from FCA (cm^{-3})	N_D from N_A-p_0 (cm^{-3})
74	0.35 ×10^{16}	nil	3.5	<10^{16}	<10^{15}	0.36×10^{16}	-	-
72	1.75×10^{16}	nil	1.1	1.2×10^{16}	<10^{15}	1.7×10^{16}	-	-
73	5.0 ×10^{16}	nil	0.44	4.2×10^{16}	<10^{15}	4.3×10^{16}	-	-
45	3.25×10^{16}	2.75×10^{16}	2.0	3.7×10^{16}	3.3×10^{16}	4.0×10^{16}	0.98×10^{16}	3.0×10^{16}
44	7.5 ×10^{16}	5.0 ×10^{16}	0.57	7.1×10^{16}	4.5×10^{16}	8.1×10^{16}	3.6×10^{16}	4.5×10^{16}

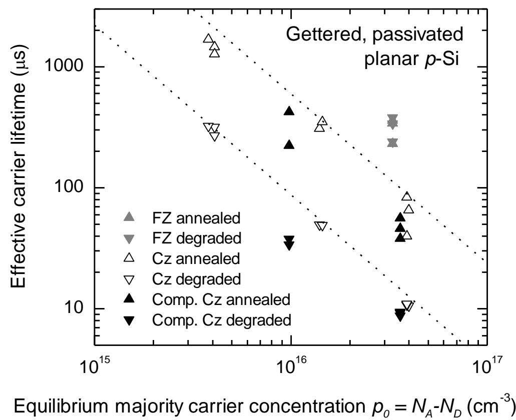

Figure 3. Effective carrier lifetimes measured at an excess carrier density of $\Delta n = 0.1\times p_0$, as a function of p_0. Lifetimes in the annealed state and after light-induced degradation are shown. The dashed lines are guides to the eye.

the net doping p_0, and also plotted against the boron concentration N_A as determined from the iron-acceptor association time $\tau_{assoc.}$

If the boron-oxygen defects were able to form with *all* of the boron in the samples, then the compensated data plotted as a function of N_A should line up with the control data. However, this is clearly not the case. In fact, the compensated data are in reasonable agreement with the control data when plotted against p_0. This implies that it is only the *uncompensated* boron that is available to form the boron-oxygen defect, or, conversely, that the excess compensated boron must be present in a form that cannot bond with oxygen dimers. This observation could be explained by the presence of B-P pairs.

3.3 The defect generation rate

Further evidence for the extent of boron-oxygen defects in compensated silicon being determined only by the net doping comes from measurements of the defect generation rate. This approach does not require knowledge of the absolute value of the lifetime or

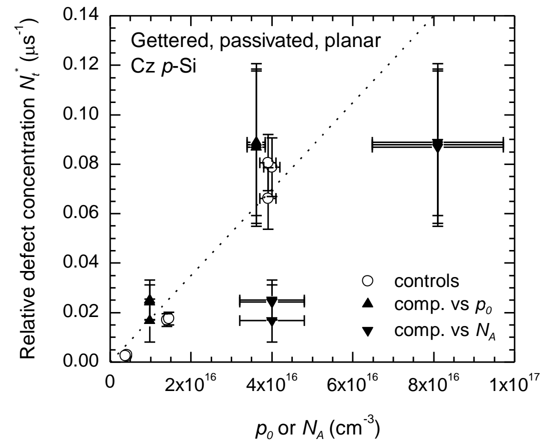

Figure 4. Relative defect concentration N_t as a function of either p_0 or N_A for both the non-compensated controls and the compensated Cz samples. The dashed line is a linear fit to the control data.*

injection level, but only a measurement of the relative change in lifetime, from which a time constant is extracted. Hence knowledge of the carrier mobilities is not required for accurate results, in contrast to the analysis above regarding the defect concentrations.

The generation rate of the boron-oxygen defect has been shown to be proportional to $p_0\times N_A$ [10]. Here, N_A is implicitly understood to mean the concentration of boron atoms *available for defect generation*. The dependence on p_0 comes from the requirement for the oxygen dimers to capture free holes to facilitate their diffusion. In compensated *p*-type silicon, if all of the phosphorus atoms are paired with boron atoms, then the amount of boron available for defect formation is simply p_0, and the generation rate will be proportional to p_0^2. On the other hand, if all of the boron is able to bond with the oxygen dimers, then the generation rate will be proportional to $p_0\times N_A$.

The generation rate of the defect R_{gen}, was determined by fitting an exponential curve to measurements of the increase in defect concentration under illumination, examples of which are shown in Figure 5. Figure 6 shows

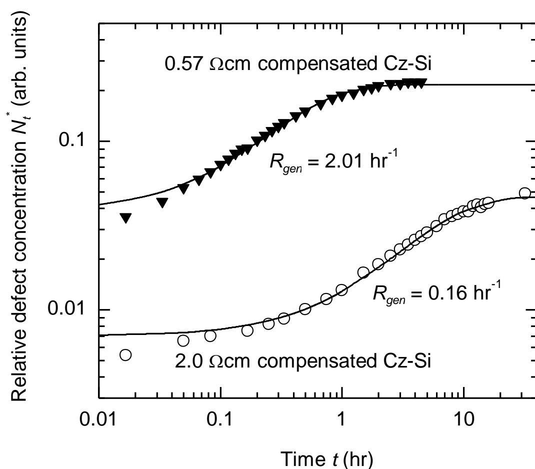

Figure 5. Relative defect concentration N_t as a function of time for two compensated samples, as the defect forms under illumination. The solid lines show fits used to determine the defect generation rates.*

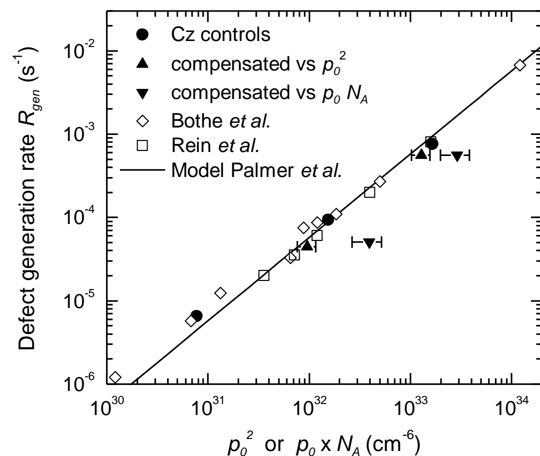

Figure 6. The defect generation rate R_{gen} as a function of p_0^2 or p_0N_A. Data for non-compensated wafers taken from Bothe et al. and Rein et al. are also shown, as is the model from Palmer et al.

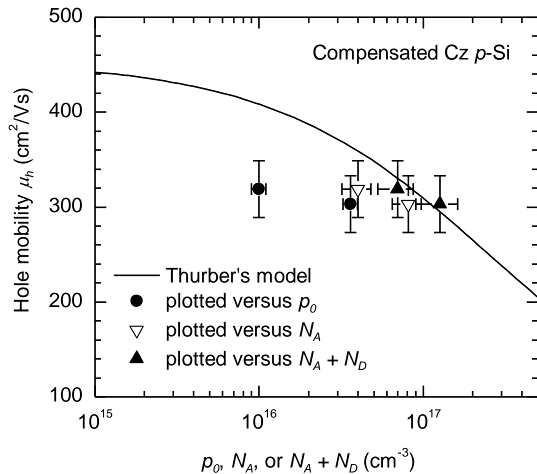

Figure 7. Majority carrier (hole) mobilities for the compensated samples plotted as a function of p_0, N_A or N_A+N_D. Thurber's mobility model is also shown.

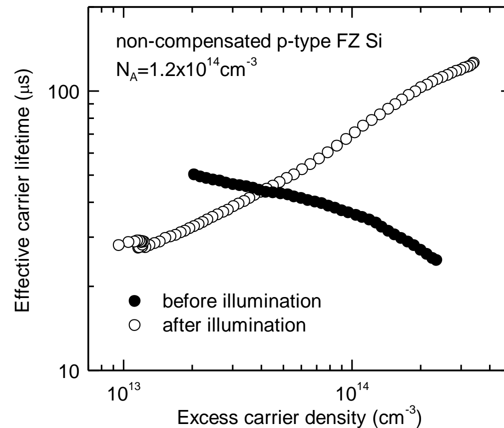

Figure 8. An example of the lifetime crossover point upon illumination of a boron-doped p-type silicon wafer containing interstitial iron. Taken from Macdonald et al. (2006).

measured defect generation rate values for the non-compensated controls, and also for the two compensated ingots, plotted either against p_0^2, or against p_0N_A. Figure 6 also shows R_{gen} data for non-compensated material taken from Bothe *et al.* [11] and Rein *et al.* [12]. The solid line represents the model of Palmer *et al.* [10]. All of the data for non-compensated silicon follows this model quite well. However, for the case of the compensated material, when plotted against p_0N_A, there is a clear discrepancy. When plotted against p_0^2, the data matches the expected model. This confirms again that it is the *net doping* which drives the formation of the defect.

At this point, one may begin to suspect that the dependence of the formation of the boron-oxygen defect on p_0, rather than the total boron concentration, reflects some underlying influence of the Fermi level, rather than the direct involvement of boron atoms in the make-up of the defect. However, it is worthwhile remembering that there is no analogue of the boron-oxygen defect observed in Ga-doped p-type Cz silicon, despite similar oxygen concentrations and Fermi levels. We therefore conclude that the compensated boron in our samples is in some chemical state that precludes it from forming the boron-oxygen defect, in much the same way that Ga does not allow the defect to be formed.

As mentioned above, one possibility for this altered state of the compensated boron dopants is the presence of B-P pairs. Such B-P pairs would also have an impact on measurable quantities such as the majority carrier mobility, and the carrier lifetime crossover point, providing an opportunity to indirectly probe for their presence, as discussed in the following sections.

3.4 Majority carrier mobilities

The presence of B-P pairs in silicon would be expected to have an impact on the carrier mobilities, since they would result in fewer charged scattering centres than in similarly doped material in which the B and P atoms were separate and ionized. If the B-P pairs are electrically neutral in thermal equilibrium, then the total concentration of charged dopant centres is simply p_0 (the concentration of unpaired B atoms). On the other hand, if they present a singly-charged centre, the total concentration of charged dopant centres is then N_A. Finally, if no B-P pairs exist, and all of the dopant atoms are separate and ionised, then this quantity would be N_A+N_D.

Figure 7 shows our measured values for the majority carrier (hole) mobility in the two compensated ingots. The solid line depicts Thurber's model [13,14], which we have preferred to Klaassens' for this purpose, because it allows an easier comparison of the different cases, without sacrificing much accuracy. When plotted as a function of p_0 the fit is poor, suggesting that neutral B-P pairs are inconsistent with our mobilities. The best agreement is obtained when plotted against N_A+N_D, for which no B-P pairs exist. Finally, when plotted against be N_A, the agreement is reasonable. This corresponds to the case when the B-P pairs are singly charged. However, we believe this is an unlikely situation, since they would then, in their own right, be either acceptor or donor states, and should therefore impact on the net doping and resistivity. Therefore, we believe our mobility data does not support the presence of B-P pairs.

3.5 The crossover point

Indirect evidence for the existence or otherwise of B-P pairs could also come from measurements of the recombination activity of iron-dopant pairs. In non-compensated boron-doped p-type silicon, the presence of FeB pairs leads to a well-known 'crossover point' in the carrier lifetime curve when the FeB pairs are dissociated by illumination. An example is shown in Figure 8, taken from Ref. [15]. In this case the crossover point occurs at an excess carrier density of around 4×10^{13}cm^{-3}. The position of this crossover point is sensitive to the recombination parameters of the FeB pairs, i.e., their energy level and capture cross sections for electrons and holes. Figure 9 shows how the position of the crossover point is expected to depend on the net doping, based on the known values of the energy level and cross sections [15]. Also shown are some measured values from the literature [15], and the values measured on the control samples of this work.

In compensated silicon, it has been established

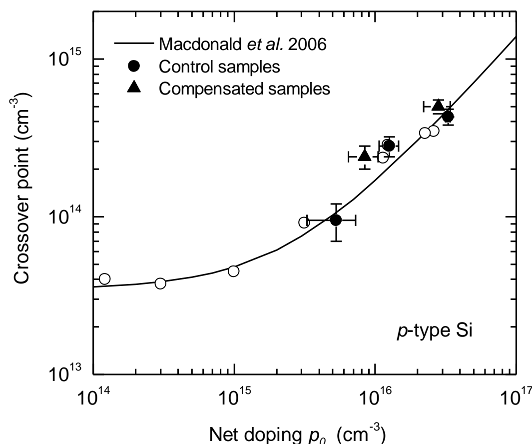

Figure 9. The position of the characteristic crossover point, as a function of the net doping, for the control samples and the compensated samples. Also shown are data and a fit from Macdonald et al. (2006).

previously that interstitial iron can pair with *all* of the B [6]. This means that if B-P pairs were present in the compensated material, a significant fraction of these FeB pairs would actually be Fe-B-P ‘triplets’. It would seem reasonable to expect these to have a different energy level and capture cross sections to normal FeB pairs. This would in turn lead to a change in the position of the crossover point.

We have measured the position of the crossover point in our compensated samples, and the results are also plotted in Figure 9. The crossover points lie close to the values for the non-compensated samples, indicating that there are no Fe-B-P complexes in these samples, or, if there are, then they must have similar recombination properties to FeB pairs. This would require a quite unlikely coincidence. This in turn casts further doubt on the existence of B-P pairs in our compensated silicon samples.

3.6 Discussion

Whatever the cause of the lower than expected activity of boron-oxygen defects in compensated *p*-type silicon, the implications for solar cells are positive. It means that already compensated feedstock can be further compensated deliberately during ingot growth to optimise the wafer resistivity for solar cell production, without the addition of extra boron-oxygen defects. Another interesting prospect is the production of compensated n-type silicon ingots from solar-grade feedstock. Even if there are significant quantities of both boron and oxygen in such wafers, they should not exhibit any boron-oxygen defects (since all of the boron is compensated).

However, one certain problem with using compensated material is the reduction in carrier mobilities. We have measured small reductions in the majority carrier mobility here (about 20%). For devices, however, the minority carrier mobility is often more important, since it determines the minority carrier diffusion length. A similar 20% reduction in the minority carrier mobility would result in a modest 10% reduction in the minority carrier diffusion length. However, the impact of compensation on minority carrier mobilities remains to be confirmed experimentally.

4 CONCLUSIONS

Measurements of boron-oxygen defect concentrations and generation rates confirmed that it is only the net doping which determines the ultimate defect concentration in compensated p-type Cz silicon, rather than the total boron concentration. However, the presence of B-P pairs as a possible explanation for these observations does not seem to be consistent with our measurements of the hole mobilities, or the characteristic crossover point caused by interstitial iron in the samples. Therefore, the physical cause of the reduced concentrations of boron-oxygen defects in compensated silicon remains unresolved. In any case, the result is a positive one for the future manufacture of solar cells from compensated feedstocks, although small reductions in carrier mobilities may have some impact on device performance.

Parts of this work have been published in Journal of Applied Physics volume 105, 093704 (2009).

Acknowledgements

This work has been supported by the Australian Research Council and the Go8/DAAD Australia Germany Joint Research Co-operation Scheme. We are grateful to Kai Petter of Q-cells for kindly supplying the wafers used in this study. Thanks are also due to Chris Samundsett for assisting with sample preparation, and Ron Sinton of Sinton Consulting for providing a QSSPC data analysis package with easily adjusted mobilities.

References

[1] J. Schmidt and K. Bothe, Physical Review B 69 (2004) 024107.

[2] R. Kopecek, J. Arumughan, K. Peter, E. A. Good, J. Libal, M. Acciarri and S. Binetti, Proceedings 23rd European Photovoltaic Solar Energy Conference, Valencia, Spain (2008) 1855.

[3] K. Bothe, R. Sinton and J. Schmidt, Progress in Photovoltaics: Research and Applications 13 (2005) 287.

[4] R. A. Sinton and A. Cuevas, Applied Physics Letters 69 (1996) 2510.

[5] M. DiSabatino, A. L. Dons, J. Hinrichs, O. Lohne and L. Arnberg, Proceedings 22nd European Photovoltaic Solar Energy Conference, Milan, Italy (2007) 271.

[6] D. Macdonald, A. Cuevas and L. J. Geerligs, Applied Physics Letters 92 (2008) 202119.

[7] D. Macdonald, F. Rougieux, A. Cuevas, B. Lim, J. Schmidt, M. DiSabatino and L. J. Geerligs, Journal of Applied Physics 105 (2009) 093704.

[8] D. B. M. Klaassen, Solid-State Electronics 35 (1992) 953.

[9] D. B. M. Klaassen, Solid-State Electronics 35 (1992) 961.

[10] D. W. Palmer, K. Bothe and J. Schmidt, Physical Review B 76 (2007) 035210.

[11] K. Bothe and J. Schmidt, Journal of Applied Physics 99 (2006) 013701.

[12] S. Rein, T. Rehrl, W. Warta, S. W. Glunz and G. Willeke, Proceedings 17th European Photovoltaic Solar Energy Conference, Munich, Germany (2001) 1555.

[13] W. R. Thurber, R. L. Mattis, Y. M. Liu and J. J. Filliben, Journal of the Electrochemical Society 127 (1980) 2291.
[14] W. R. Thurber, R. L. Mattis, Y. M. Liu and J. J. Filliben, Journal of the Electrochemical Society 127 (1980) 1807.
[15] D. Macdonald, T. Roth, P. N. K. Deenapanray, T. Trupke and R. A. Bardos, Applied Physics Letters 89 (2006) 142107.